ACS Catalysis

Research Article

pubs.acs.org/acscatalysis

Benzyne Formation in the Mechanism-Based Inactivation of Cytochrome P450 by 1-Aminobenzotriazole and *N*-Benzyl-1-Aminobenzotriazole: Computational Insights

Pratanphorn Chuanprasit,[†] Shu Hui Goh,[†] and Hajime Hirao*

Division of Chemistry and Biological Chemistry, School of Physical and Mathematical Sciences, Nanyang Technological University, 21 Nanyang Link, Singapore 637371

Supporting Information

ABSTRACT: Cytochrome P450 enzymes (P450s) are ubiquitously distributed heme enzymes that play catalytic roles in the essential oxidative biotransformation of a wide range of exogenous and endogenous organic compounds. Strong inhibition of P450s through mechanism-based inactivation (MBI) essentially should not occur, because it would affect important metabolic processes adversely. However, accumulated evidence shows that the MBI of a P450 is not a rare event. MBI can also be exploited for useful applications such as reaction phenotyping. Thus, MBI is clearly one of the major problems concerning P450s, but the reaction mechanisms underlying MBI are not very clear in many cases. In this work, we used density functional theory (DFT) calculations to understand how a metabolite (benzyne) is formed from two mechanism-based inactivators of P450s: 1-aminobenzotriazole (ABT) and *N*-benzyl-1-aminobenzotriazole (BBT). ABT has been widely used for reaction phenotyping. Our DFT calculations show that the formation of benzyne from ABT occurs via two sequential H-abstraction reactions from the exocyclic N−H bonds, similar to the reaction of 1,1-dimethylhydrazine (Hirao, H.; Chuanprasit, P.; Cheong, Y. Y.; Wang, X. *Chem. Eur. J.* **2013**, *19*, 7361−7369). The transition states for these H-abstractions are stabilized by a proton-coupled electron transfer effect. The formation of benzyne from BBT is also triggered by H-abstraction from the N−H bond. However, in this case, the second step is H-abstraction from a benzylic C−H bond. In addition, for the formation of benzyne from BBT, another catalytic cycle should be necessary. Our computational study therefore elucidates the difference in reaction mechanisms between ABT and BBT, providing new insights into the processes involved in the MBI caused by these compounds.

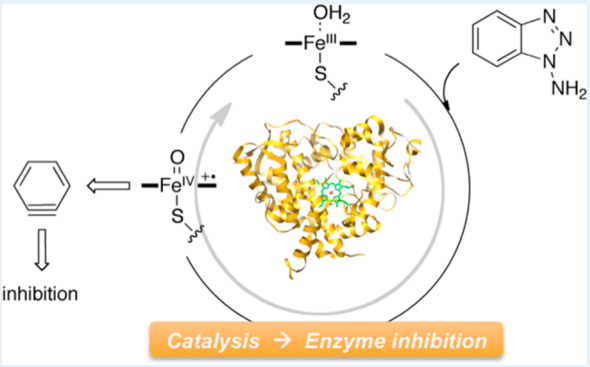

KEYWORDS: *cytochrome P450, mechanism-based inactivation, density functional theory, benzyne, reaction mechanism*

1. INTRODUCTION

The intensive investigations into cytochrome P450 enzymes (P450s) over the past more than 50 years have shown that P450s are ubiquitous in organisms, including bacteria, insects, plants, and mammals, to assist the oxidative biotransformation of exogenous and endogenous compounds, and that different P450s share significant degrees of structural and mechanistic similarities.[1−12] For example, P450s utilize a cysteine-ligated heme cofactor for catalysis, and the ways they operate in catalytically oxidizing organic substrates are essentially the same in the majority of cases. However, in view of the practical implications of P450s, especially in the context of their ability to metabolize a significant number of drugs, our current understanding of P450s could arguably be said to remain far from complete. For such enzymes, one must have in-depth knowledge of the reactivity and specificity in the substrate oxidation of individual enzymes, but compared with the number of known sequences of P450s (>18 000), the number of P450s, for which the mechanism and function are fully understood, is much smaller.[6,7]

Besides their mechanisms for substrate oxidation, mechanism-based inactivation (MBI) of P450s also merits further investigation, especially because of the widespread roles played by P450s in pharmacology and toxicology. Numerous reviews have been written about MBI by research groups in academia[13−18] and industry.[19−22] MBI impairs the metabolic function of P450s, thereby often causing unwanted outcomes. Thus, metabolic clearance of a drug may be reduced by another compound (mechanism-based inactivator) that inhibits a P450, or the drug itself may act as a mechanism-based inactivator to affect adversely the metabolism of other compounds. Gaining molecular-level understanding of the mechanisms underlying MBI will certainly be beneficial in predicting and minimizing

Received: February 26, 2015
Revised: March 30, 2015
Published: March 31, 2015

DOI: 10.1021/acscatal.5b00423
ACS Catal. 2015, 5, 2952−2960

issues associated with liabilities to MBI. However, the detailed mechanisms are not necessarily clear for most of the known MBI processes. This is mainly because MBI involves a chemical reaction mediated by the P450 eventually inactivated, and experimentally tracing all the rapid reaction steps involved is virtually impossible. Moreover, accurate description of the reactive process is beyond the capabilities of classical force-field-based computational methods, which are often utilized in drug discovery projects. Motivated by the belief that quantum mechanical computational approaches such as density functional theory (DFT) should provide us with valuable insights into reactions in MBI, we have studied several MBI processes using DFT over the past few years.[23−25] Other investigators have also examined MBI processes computationally.[26−29]

MBI also has useful applications such as *in vitro* reaction phenotyping[30−32] and *in vivo* identification of the organ contributing to drug metabolism.[33] These methods are useful because it is often unclear which P450 metabolizes a given substrate or where in the body P450-mediated drug metabolism takes place. For these applications, 1-aminobenzotriazole (ABT) has been widely used as an inactivator of many P450 isozymes (Scheme 1).[32] The pioneering work done by Ortiz de

Scheme 1. ABT and BBT

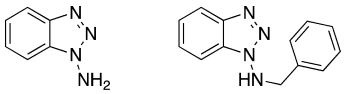

Montellano and co-workers has shown that benzyne, which is generated from ABT during catalytic turnover in a P450, forms covalent bonds with two vicinal nitrogen atoms of protoporphyrin IX.[34−36] Furthermore, Mathews and Bend reported that the same *N*-alkylated product was formed *in vivo*, when phenobarbital-treated rats were treated with an ABT analogue, *N*-benzyl-1-aminobenzotriazole (BBT, Scheme 1).[37] It should be noted that in the case of the MBI by BBT, instead of benzyne formation, somewhat different trends were observed, for example, in the guinea pig hepatic and pulmonary microsomes, indicating that the benzyne formation is not necessarily the only channel for the reaction of BBT.[38−40] Nevertheless, in regard to the MBI caused by ABT and BBT, it seems to us that the formation of benzyne is a key reaction, the mechanism of which should be understood first, before other possible mechanisms are explored.

For the reaction of ABT, it is often postulated that benzyne is formed via either path A or B as illustrated in Scheme 2. Thus, ABT may undergo two sequential H-abstraction steps (path A) or *N*-hydroxylation (path B) after a H-abstraction step. In either pathway, a nitrene species is formed, and this species is decomposed into benzyne and two nitrogen molecules. In addition to these pathways, path C, which begins with *N*-oxidation, may also be possible. In path C, the lone-pair orbital of the exocyclic amine of ABT attacks the oxo moiety of the compound I (Cpd I) reactive intermediate, and an *N*-hydroxylated intermediate is formed in the same way as in path B. Although these possible mechanisms could be envisaged for the MBI by ABT, it is not yet clear exactly how benzyne is formed. Therefore, the goal of this study was to identify the most plausible mechanism for this benzyne-forming reaction. Furthermore, attempts were made to understand how benzyne is formed from BBT. For these purposes, we use a DFT computational approach.

2. METHOD

All DFT calculations were performed using Gaussian 09.[41] A simple model of Cpd I was used, which consists of oxoiron(IV), doubly deprotonated porphine (to represent protoporphyrin IX), and HS^- (to represent a cysteinate ligand). The B3LYP/

Scheme 2. Possible Pathways of Benzyne Formation from ABT: (a) Path A, (b) Path B, and (c) Path C[a]

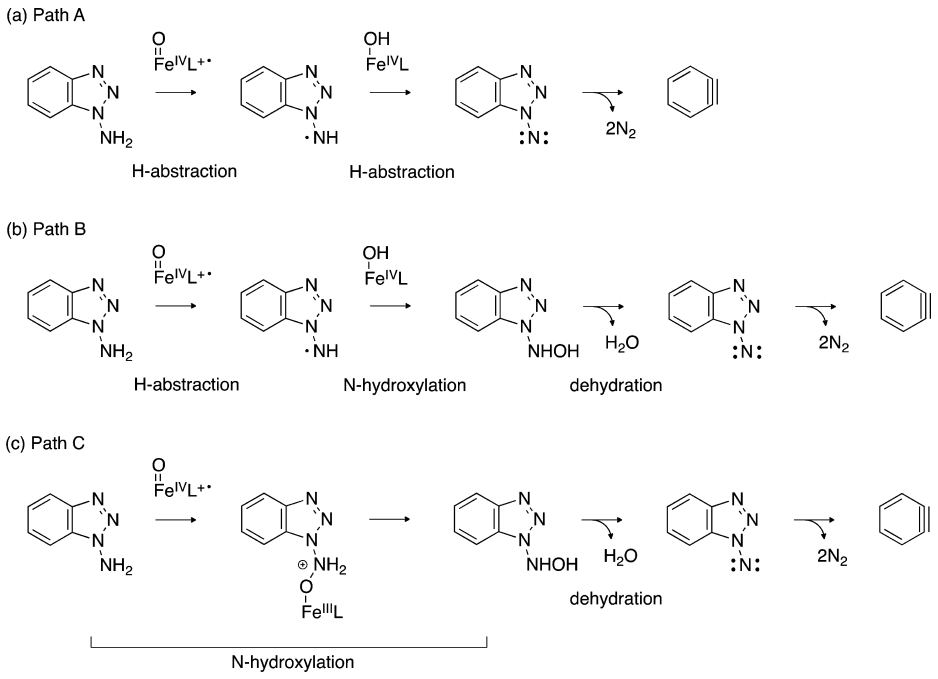

[a]L stands for the porphyrin ligand of a P450.

DOI: 10.1021/acscatal.5b00423
ACS Catal. 2015, 5, 2952−2960

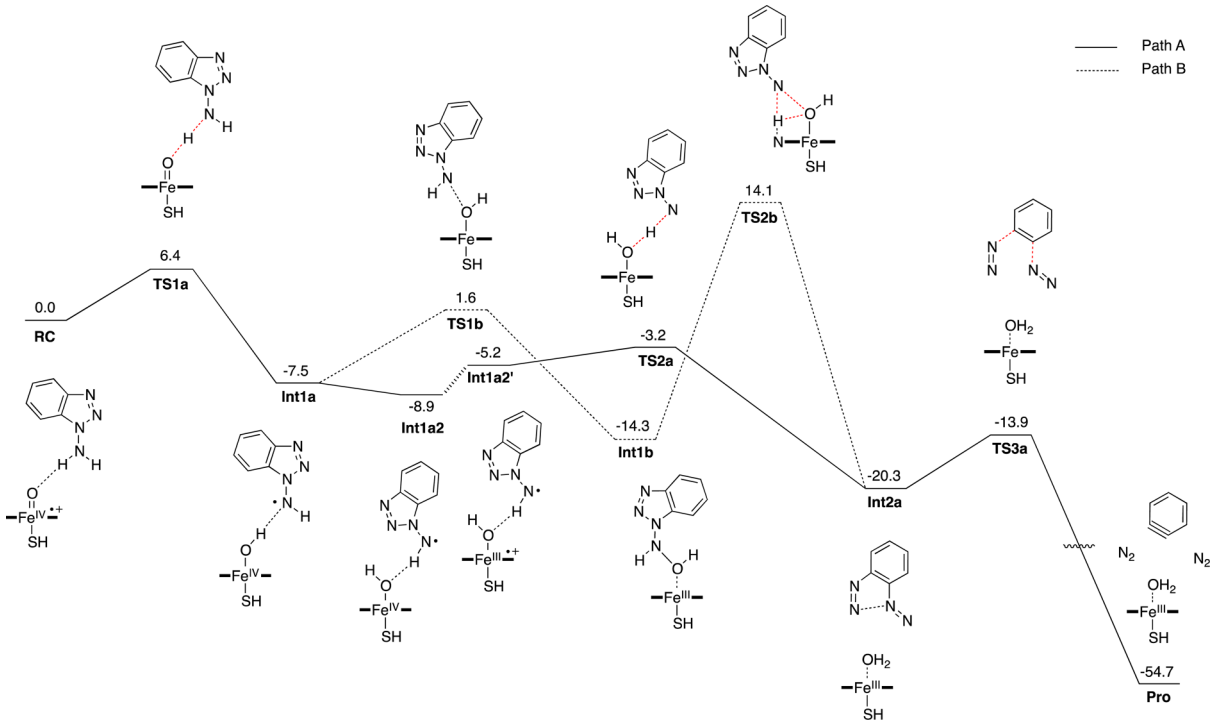

Figure 1. Energy profiles (kcal/mol) for the reaction of ABT (paths A and B), as determined at the B3LYP(SCRF)/B2//B3LYP/B1+ZPE level.

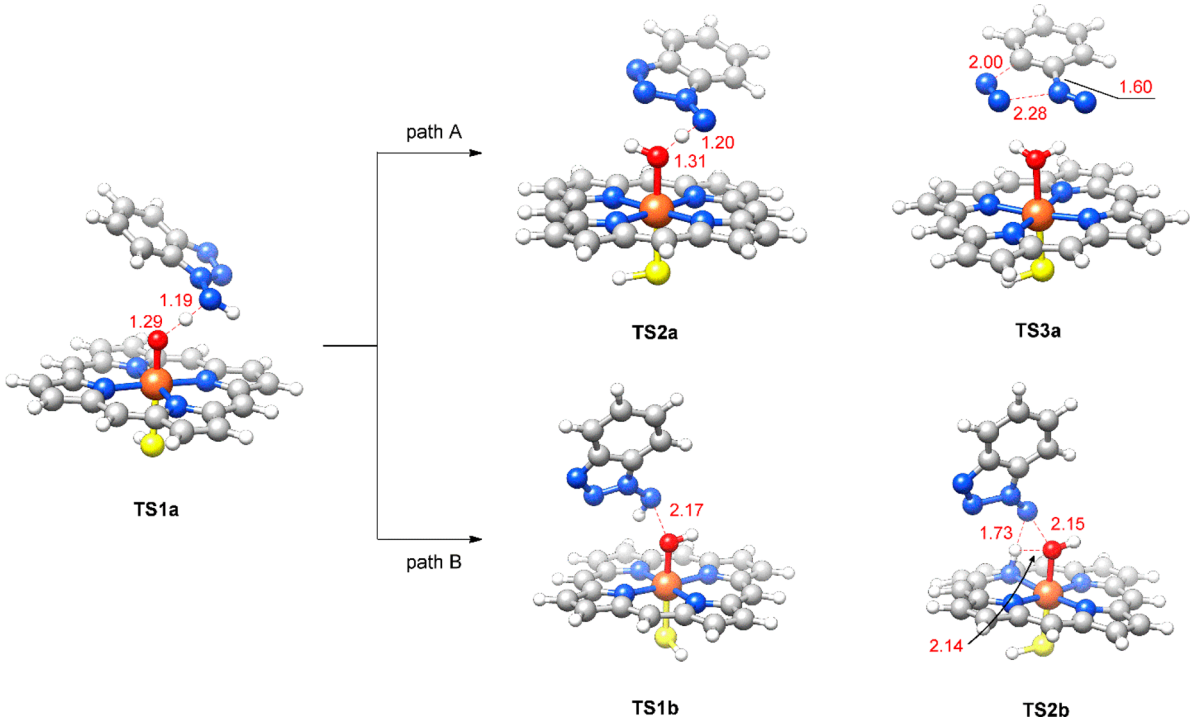

Figure 2. Optimized TS geometries for paths A and B of the reaction of ABT. Key bond distances are shown in Å.

[SDD(Fe),6-31G*(others)] method was used for geometry optimization and frequency calculations,[42−46] and the B3LYP-(SCRF)/6-311+G(d,p) method was used for subsequent energy refinement.[47−49] For simplicity, [SDD(Fe),6-31G*-(others)] will be henceforth called B1, and 6-311+G(d,p) will be called B2. The frequency calculations with B1 yielded zero-point energy (ZPE) values, which were added to the electronic energies to obtain final energy values. Based on the assumption that the polarizability of a protein media should be close to that in a chlorobenzene solvent, the effect of a chlorobenzene solvent (ε = 5.6968) was included in the latter calculation using a self-consistent reaction field (SCRF) method called IEFPCM.[50] The low-energy doublet spin state was considered when studying reaction mechanisms. The B3LYP functional has been shown to describe the energetics of P450 systems reasonably well.[8−10] Time-dependent DFT (TDDFT) calculations were also performed for selected species at the B3LYP(SCRF)/B2 level, to assess the plausibility of electron

DOI: 10.1021/acscatal.5b00423
ACS Catal. 2015, 5, 2952−2960

transfer. G4 enthalpy calculations were also performed for ABT, to evaluate its homolytic N−H bond dissociation energy (BDE).[51] BDE data generally correlate very well with H-abstraction barrier heights.[52] Chimera was used to draw three-dimensional molecular structures,[53] and Molekel was used to plot orbitals.[54]

3. RESULTS AND DISCUSSION

3.1. Formation of Benzyne from ABT. Both paths A and B (Scheme 2) begin with H-abstraction from the exocyclic amine moiety of ABT; thus, the first H-abstraction step is shared by these pathways. Computationally determined energy profiles for these two pathways are shown in Figure 1. Optimized geometries of the transition states (TS's) for these two pathways are shown in Figure 2. In our recent study, the homolytic BDE for 1,1-dimethylhydrazine (UDMH) was calculated as 80.2 kcal/mol using the G4 method.[54] The BDE for ABT was calculated here as 83.6 kcal/mol with the same method, which suggests that the ABT is less reactive than UDMH. Indeed, the barrier for the first H-abstraction step via **TS1a** (Figure 2), i.e., 6.4 kcal/mol, is somewhat higher than that for UDMH (−0.1 kcal/mol).[24] At the stage of the initially formed reactant complex (**RC**), the Cpd I moiety has a triradicaloid character, with two unpaired electrons occupying two π^* orbitals and one unpaired electron occupying the a_{2u}-type orbital (see Scheme 3). The H-abstraction results in the formation of intermediates (**Int1a** and then **Int1a2**) on the reaction pathway. During the H-abstraction, one electron is shifted from ABT to the a_{2u} orbital of Cpd I, and therefore, the a_{2u} orbital of these intermediates is doubly occupied. The same trend was observed previously for the H-abstraction from UDMH.[24,55] If **Int1a2** undergoes a second H-abstraction reaction, an electron transfer should occur from the ABT fragment to the π^* orbital of the iron center. A pathway involving this electronic reorganization could not be obtained. However, if the electronic occupation of **Int1a2** is changed by an electron transfer from a_{2u} to π^*, the resultant species **Int1a2′** can undergo H-abstraction with a tiny energy barrier via **TS2a**, to form **Int2a**. The electron transfer from a_{2u} to π^* does not seem to be a difficult process, because it requires an energy cost of only 3.7 kcal/mol. Interestingly, the N1−N2 bond in **Int2a** is almost cleaved, and conversion of **Int2a** into the product complex (**Pro**) involves decomposition of the substrate moiety in this intermediate into benzyne and two nitrogen molecules. This step had a barrier of only 6.4 kcal/mol. Thus, overall, the benzyne formation via path A does not have any unusually high barriers.

Scheme 3. Schematic Electron Occupation Diagram for Cpd I in the Doublet State

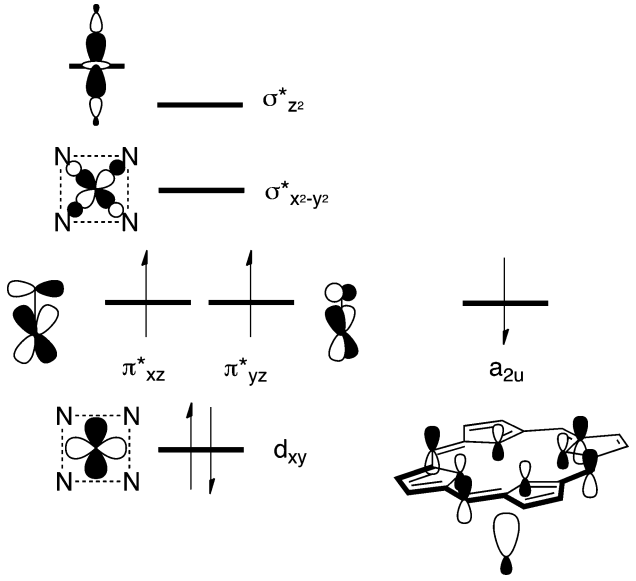

By contrast, on path B, **Int1a** undergoes *N*-hydroxylation through a TS for N−O bond formation (**TS1b**, Figure 2). The *N*-hydroxylation step has a barrier of 9.1 kcal/mol, which is higher than that for the H-abstraction from **Int1a2** via **Int1a′** and **TS2a** by a few kcal/mol. Hence, calculations suggest that path B should be less favorable than path A. Furthermore, even if *N*-hydroxylation is completed and **Int1b** is formed, path B must surpass a very high barrier (28.4 kcal/mol) in the next step to form the nitrene intermediate **Int2a**, via proton transfer from ABT to the hydroxyl group using one of the pyrrole nitrogen atoms of the porphyrin ligand (**TS2b**, Figure 2).[27,56] Therefore, these comparative analyses of paths A and B lead us to suggest that benzyne formation via path B is not plausible and that the reaction should preferentially follow path A when forming benzyne from ABT.

As we have seen in Figure 1, the more favorable path A contains two sequential H-abstraction steps. When an oxoiron(IV) species abstracts a hydrogen atom from an X−H bond (X = N or O), the reaction tends to exhibit a proton-coupled electron transfer (PCET) character.[57] In addition, when the PCET character is dominant in the H-abstraction process, a spin natural orbital (SNO) is not localized onto the breaking X−H bond; rather, it has a lone-pair-like orbital amplitude. This pattern is different from what is observed for pure hydrogen-atom-transfer processes. Interestingly, as shown in Figure 3, the SNOs for both **TS1a** and **TS2a** show the amplitude pattern of PCET, with the orbitals having a significant lone-pair character, instead of having a σ(N−H) character. Thus, both of the two H-abstraction steps in the reactions of ABT may be characterized as PCET processes. In general, the PCET effect lowers the barrier height for H-abstraction to some extent.[57] As mentioned above, the homolytic BDE for ABT was 83.6 kcal/mol, and the barrier for the first H-abstraction is 6.4 kcal/mol. Using the calibration plot presented in our recent study,[55] the TS stabilization because of PCET is estimated to be about 4 kcal/mol in the case of ABT.

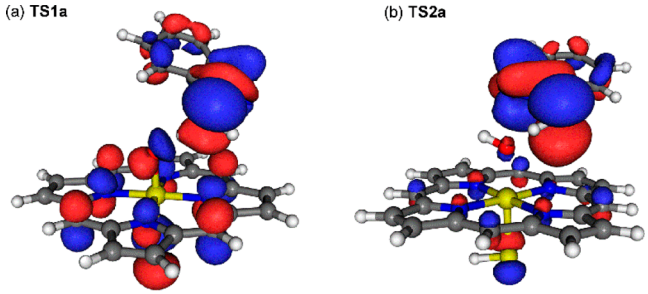

Figure 3. Spin natural orbitals (B3LYP/B1) for (a) **TS1a** and (b) **TS2a**.

Another interesting finding in the reaction pathway analyses for ABT is that the N1−N2 bond is almost cleaved in the nitrene species at the stage of **Int2a**, and it looks somewhat

DOI: 10.1021/acscatal.5b00423
ACS Catal. 2015, 5, 2952−2960

different from the structure in the conventional hypothesis, which assumed that the N1−N2 bond remains at this stage (see Scheme 2). An analysis of the spin density distribution showed that the nitrene moiety in **Int2a** did not have a radical character but rather had a closed-shell singlet character. As it might be that the nitrene species actually has a triplet ground state, we performed additional calculations on the isolated nitrene in the singlet and triplet states. The optimized structures of nitrene are shown in Figure 4. The calculations showed that in the triplet state, the N1−N2 distance (2.77 Å) is much greater than that for the singlet state (1.97 Å), because of the spin localization on nitrogen atoms in the triplet state. However, the singlet state was more stable than the triplet state by 1.1 kcal/mol (Figure 4). In addition, the dissociation of two nitrogen molecules from the nitrene species produces molecules in the singlet state; thus, following the triplet energy surface may not be very beneficial for the reaction. It is therefore likely that the nitrene species has the singlet spin state throughout the process between **Int2a** and **Pro**.

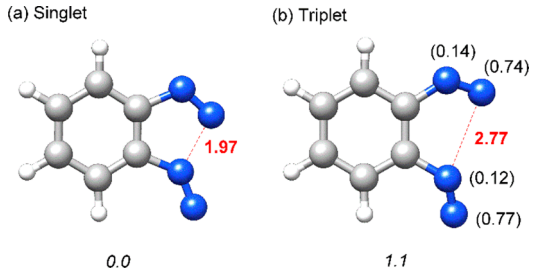

Figure 4. B3LYP/B1-optimized geometries of the nitrene species in **Int2a** in the (a) singlet and (b) triplet states. The N1−N2 distances (in Å) are shown in red, and the relative energies evaluated at the B3LYP(SCRF)/B2//B3LYP/B1+ZPE level are shown in italic font. For the triplet species, the B1 spin population values are shown in parentheses.

The energy profile for another possible pathway, path C, was also determined (Figure 5). Unlike the other pathways, path C begins with the attack of the exocyclic nitrogen of ABT on the oxoiron(IV) moiety of Cpd I, which results in a double electron transfer from ABT to Cpd I, to form **Int1c**. However, as the energy diagram shows, the barrier for this process (22.3 kcal/mol) is much higher than that for the H-abstraction barrier in the first step of paths A and B (6.4 kcal/mol, see Figure 1). If an **Int1c** happens to be formed on path C, a *N*-hydroxylated intermediate, **Int3c**, can easily be formed in a proton-shuttle mechanism using the porphyrin ligand.[27,56] **Int3c** is equivalent to **Int1b** on path B, which means that path C is later merged into path B. As we have seen in Figure 1, **Int1b** must surpass a barrier of 28.4 kcal/mol to form benzyne, and this barrier is too high. Therefore, involvement of path C in the benzyne formation from ABT does not seem likely.

3.2. Formation of Benzyne from BBT. We next explored the pathway for benzyne formation, in the reaction between BBT and P450 Cpd I. Because the *N*-oxidation pathway has a much higher barrier than the other pathways in the reaction of ABT, this pathway was not considered here. Figure 6 summarizes the calculated energy profiles for the reaction of BBT. Key TS's are also depicted in Figure 7. The barrier for H-abstraction from the N−H bond (6.4 kcal/mol) is as low as that for the ABT reaction, indicating that the benzyne formation may also begin with H-abstraction from the N−H bond in the case of BBT. The TS for H-abstraction (**TS1a-II**) in Figure 7 looks similar to that for the ABT reaction (**TS1a**). It may also be possible that hydrogen is abstracted instead from the adjacent benzylic C−H bond of BBT. Therefore, we also examined this possibility; however, the barrier for this C−H activation pathway was much higher (16.0 kcal/mol). Thus, the

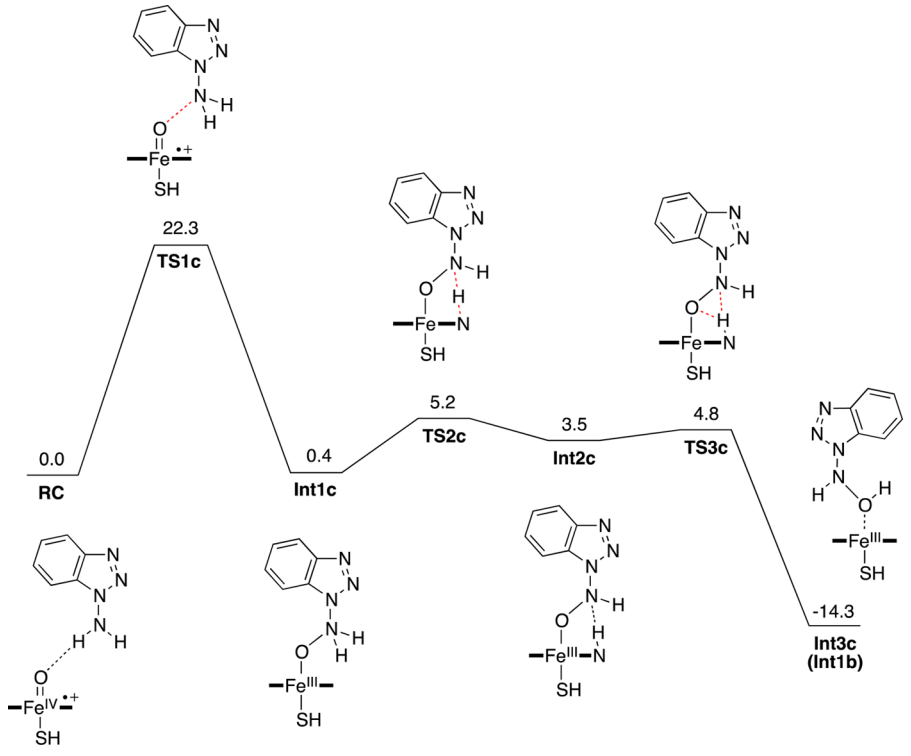

Figure 5. Energy profile (kcal/mol) for the reaction of ABT (path C), as determined at the B3LYP(SCRF)/B2/B3LYP/B1+ZPE level.

DOI: 10.1021/acscatal.5b00423
ACS Catal. 2015, 5, 2952−2960

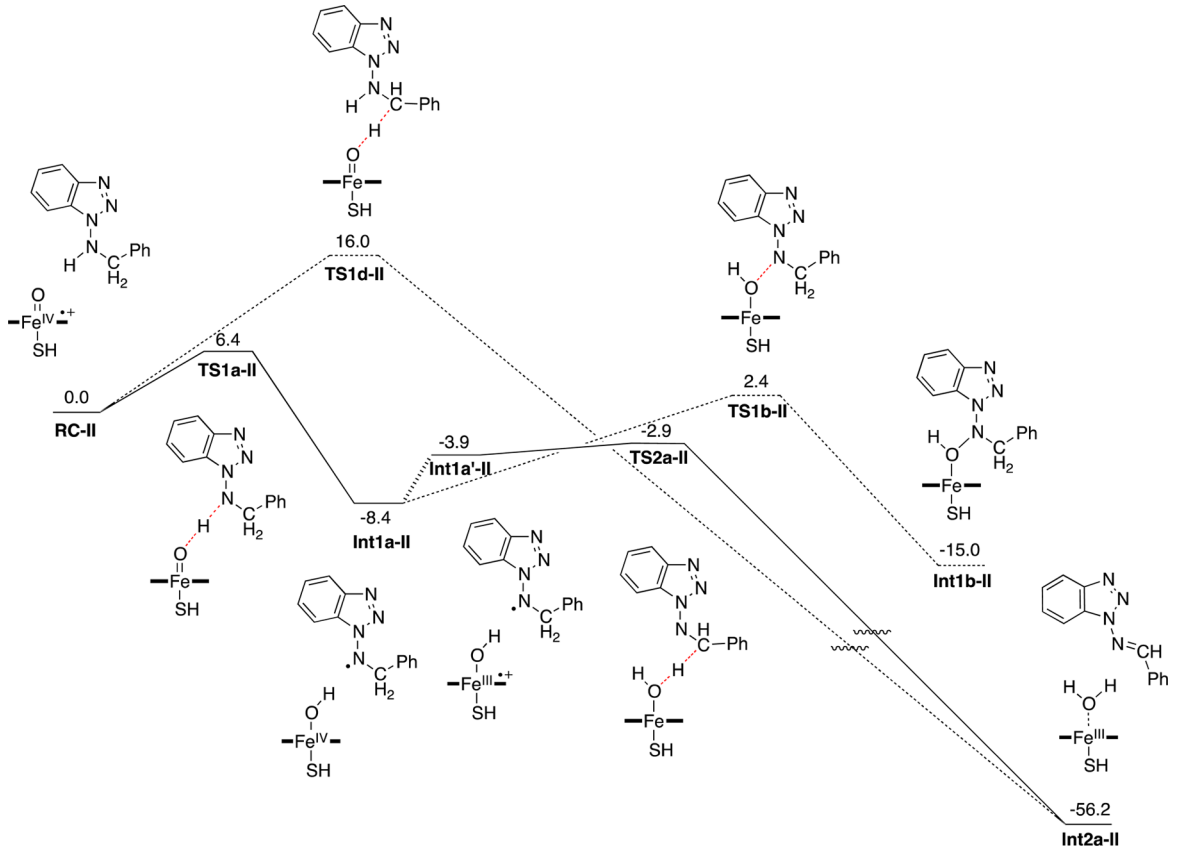

Figure 6. Energy profiles (kcal/mol) for the first step of the reaction of BBT, as determined at the B3LYP(SCRF)/B2/B3LYP/B1+ZPE level.

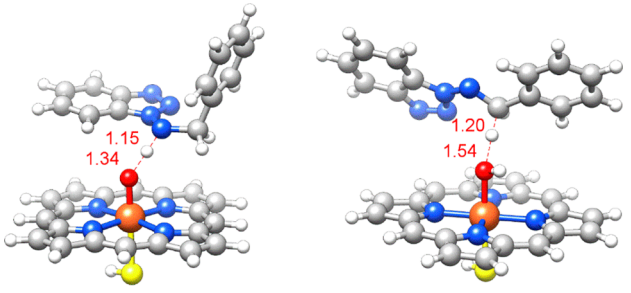

Figure 7. Optimized TS geometries for the first step of the reaction of BBT. Key bond distances are shown in Å.

first step for the BBT reaction should be H-abstraction from the N−H bond.

Unlike ABT, BBT does not have two hydrogen atoms at the exocyclic amine. Therefore, sequential H-abstraction from the amine is not possible here. The H-abstracted intermediate **Int1a-II** may undergo either *N*-hydroxylation or H-abstraction from the benzylic C−H bond. Here again, it was necessary for **Int1a-II** to undergo electron transfer from a_{2u} to the iron to produce **Int1a′-II**, before the H-abstraction from the C−H bond takes place. It was found that the barrier for H-abstraction from the benzylic C−H bond (5.5 kcal/mol) via **TS2a-II** (Figure 7) is lower than that for *N*-hydroxylation (10.8 kcal/mol) by a few kcal/mol. Thus, *N*-hydroxylation is not a favorable mechanism, and this trend is the same as that observed for ABT. As a result of the H-abstraction from the C−H bond, intermediate **Int2a-II** is formed. The same intermediate can also be formed if the first step is H-abstraction from the C−H bond via **TS1d-II**, although this pathway is less favorable, as we have seen above. The hydrazone-type molecule in **Int2a-II** has strong covalent bonds within the molecule and thus did not seem to undergo noncatalytic decomposition into benzyne. Therefore, we hypothesized that another catalytic cycle allows the hydrazone to react with Cpd I to form benzyne.

The energy profile for this mechanism is shown in Figure 8, and the optimized geometries of key TS's are displayed in Figure 9. If Cpd I species is formed in a second catalytic cycle (**RC2-II**), the hydrazone species can attack the oxo moiety of Cpd I to form a new C−O bond (**Int3a-II**) via **TS3a-II** (Figure 9). The barrier for this process was calculated as 16.3 kcal/mol, which is not too high. **Int3a-II** then easily undergoes C−N bond cleavage via **TS4a-II** (Figure 9) to form benzaldehyde and a nitrene species, and the latter was also seen in the reaction of ABT at **Int2a** (Figure 1). Thus, in the same way as the reaction of ABT, this nitrene in **Int4a-II** can be broken down easily to generate a benzyne and two nitrogen molecules. Our calculations therefore show that benzyne can be formed after two catalytic cycles in the case of BBT.

Interestingly, we also found another pathway in which **Int3a-II** undergoes ring closure to form an oxaziridine species at **Int4a′-II**, although the barrier for this process was slightly higher than that for the nitrene formation pathway. It has been shown by Bend and co-workers that in some P450 systems, the major mechanism of MBI by BBT is not heme *N*-alkylation via benzyne formation but modification of the apoprotein.[38−40] The exact mechanism of apoprotein modification remains unclear. Although this type of irreversible MBI is beyond the

DOI: 10.1021/acscatal.5b00423
ACS Catal. 2015, 5, 2952−2960

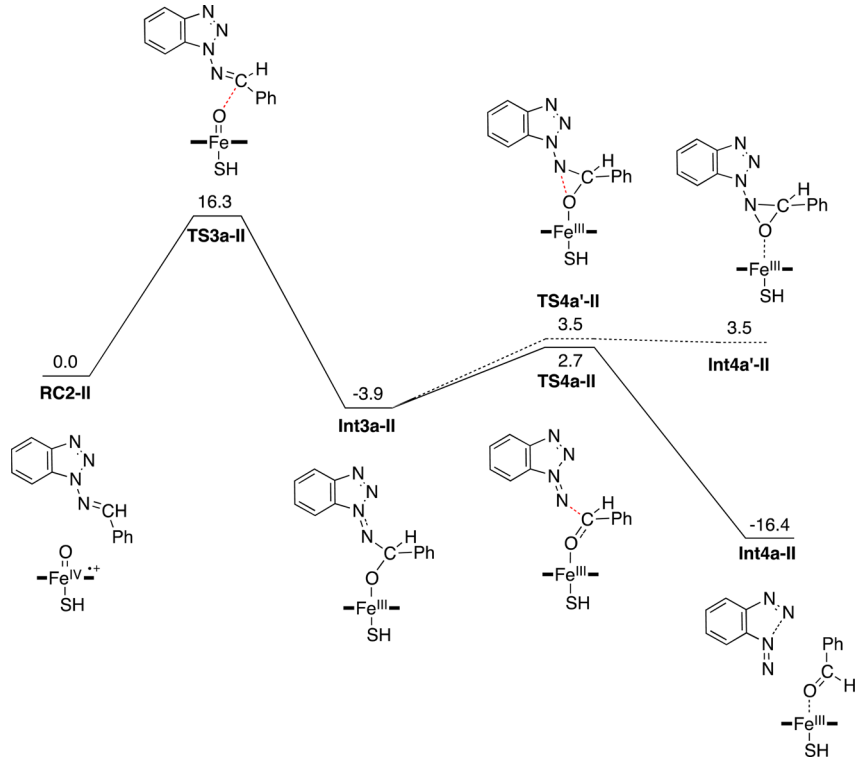

Figure 8. Energy profiles (kcal/mol) for the second step of the reaction of BBT, as obtained at the B3LYP(SCRF)/B2/B3LYP/B1+ZPE level.

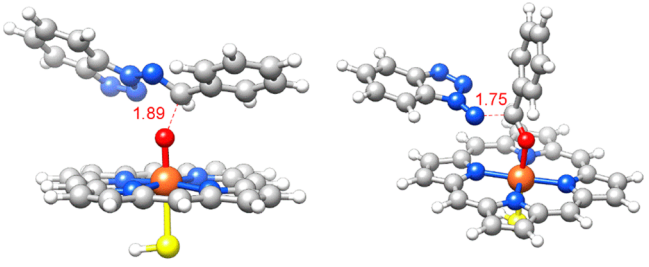

Figure 9. Optimized TS geometries for the second step of the reaction of BBT. Key bond distances are shown in Å.

scope of this study, the oxaziridine species might be involved in the apoprotein modification or other reaction channels of BBT. Note that the intermediacy of oxaziridine, which is capable of forming a covalent bond with DNA, was proposed in the reaction of a 3-substituted indazole compound, mediated by several rat P450 enzymes such as CYP3A1 and CYP3A2 (Scheme 4).[58]

Scheme 4. Previously Proposed Oxaziridine Formation during the P450-Mediated Reaction of an Indazole-Type Compound[58]

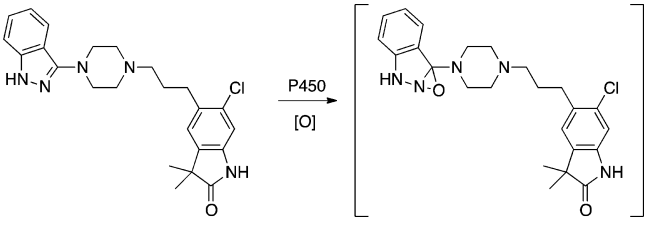

3.3. Possibility of an Electron-Transfer Mechanism.

The possibility of an electron transfer in the **RC** state for the ABT reaction and the **RC-II** state for the BBT reaction was examined by performing TDDFT calculations at the B3LYP-(SCRF)/B2 level. The importance of such an electron transfer mechanism has been suggested for other heme and nonheme iron systems.[59−61] Figure 10 depicts the key molecular orbitals that may be involved in the electron transfer or excitation from the substrate to Cpd I for the ABT reaction. The excitation energies were calculated by TDDFT as 28.6 kcal/mol for **RC** and 28.5 kcal/mol for **RC-II**. These values are much larger than the barrier height (6.4 kcal/mol) for the H-abstraction from the N−H bond of ABT or BBT (Figures 1 and 6), thus leading us to conclude that for the benzyne formation reactions of ABT and BBT, the H-abstraction mechanisms presented above should be more favorable than the electron-transfer-driven mechanism.

4. CONCLUSION

In conclusion, we have performed DFT calculations to investigate the reaction mechanism of benzyne formation from ABT and BBT, which is a critical step before the heme *N*-alkylation of a P450 enzyme through MBI. Several new insights could be derived from our computational study. The benzyne formation from ABT should take place via two sequential H-abstraction steps, in much the same way as in the reaction of UDMH. Other possible mechanisms involving *N*-hydroxylation and *N*-oxidation do not appear to be plausible because they contain very high energy barriers. The resultant nitrene species, generated after two H-abstraction steps, is easily decomposed into benzyne and two nitrogen molecules. In addition, the H-abstraction steps have a PCET character, which should lower the barrier heights to some extent. The reaction of BBT is also initiated by H-abstraction from the exocyclic amine. However,

DOI: 10.1021/acscatal.5b00423
ACS Catal. 2015, 5, 2952−2960

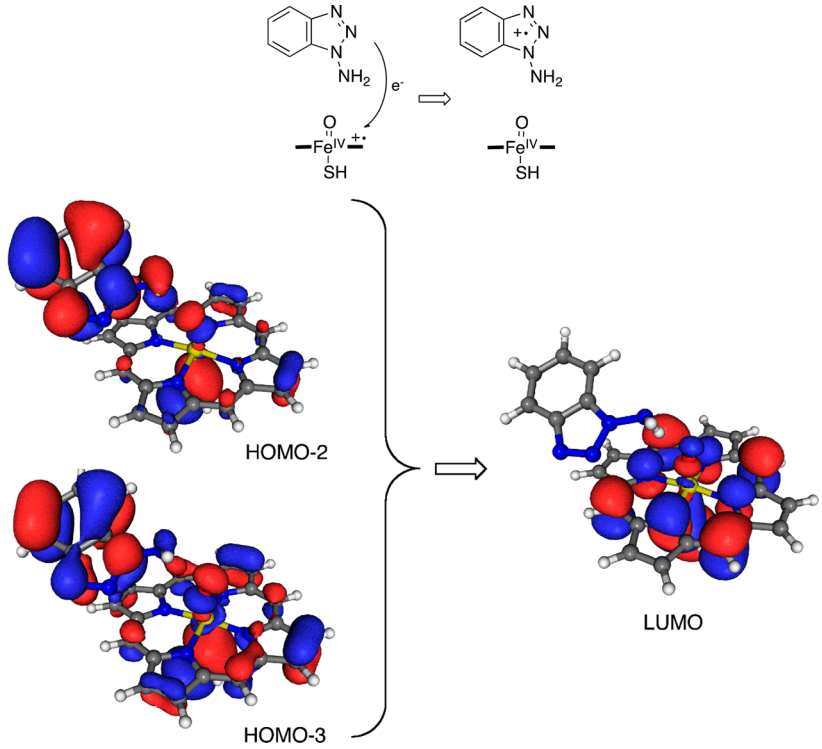

Figure 10. Orbitals relevant to electron transfer: the π-type molecular orbitals (HOMO−2 and HOMO−3) and the a_{2u}-type orbital (LUMO) for the **RC** state of ABT reaction.

in this reaction, the first H-abstraction is followed by H-abstraction from the benzylic C−H bond, because of the lack of a second hydrogen atom on the amine to be abstracted. The two H-abstraction reactions result in the formation of a hydrazone molecule, and benzyne formation from the hydrazone should require another catalytic turnover. We also examined the electron-transfer-driven mechanism, but this mechanism was not energetically favorable when compared with the H-abstraction mechanism. Thus, overall, this study has shown, in accordance with the pattern that we have observed in our recent studies on nitrogen-containing molecules with P450 Cpd I, that H-abstraction is the most important reaction in the formation of benzyne.

■ ASSOCIATED CONTENT

Supporting Information

The following file is available free of charge on the ACS Publications website at DOI: 10.1021/acscatal.5b00423.

Raw energy data and XYZ coordinates of optimized geometries (PDF)

■ AUTHOR INFORMATION

Corresponding Author

*E-mail: hirao@ntu.edu.sg.

Author Contributions

†P.C. and S.H.G. contributed equally to this work.

Notes

The authors declare no competing financial interest.

■ ACKNOWLEDGMENTS

This work was supported by a Nanyang Assistant Professorship. We thank the High Performance Computing Centre at Nanyang Technological University for computer resources.

■ REFERENCES

(1) Omura, T.; Sato, R. *J. Biol. Chem.* **1962**, *237*, 1375−1376.
(2) *Cytochrome P450: Structure, Mechanism, and Biochemistry*, 3rd ed.; Ortiz de Montellano, P. R., Ed.; Kluwer Academic/Plenum Press: New York, 2005.
(3) Sono, M.; Roach, M. P.; Coulter, E. D.; Dawson, J. H. *Chem. Rev.* **1996**, *96*, 2841−2887.
(4) Denisov, I. G.; Makris, T. M.; Sligar, S. G.; Schlichting, I. *Chem. Rev.* **2005**, *105*, 2253−2278.
(5) Sligar, S. G.; Makris, T. M.; Denisov, I. G. *Biochem. Biophys. Res. Commun.* **2005**, *338*, 346−354.
(6) Guengerich, F. P.; Munro, A. W. *J. Biol. Chem.* **2013**, *288*, 17065−17073.
(7) Poulos, T. L. *Chem. Rev.* **2014**, *114*, 3919−3962.
(8) Meunier, B.; de Visser, S. P.; Shaik, S. *Chem. Rev.* **2004**, *104*, 3947−3980.
(9) Shaik, S.; Kumar, D.; de Visser, S. P.; Altun, A.; Thiel, W. *Chem. Rev.* **2005**, *105*, 2279−2328.
(10) Shaik, S.; Cohen, S.; Wang, Y.; Chen, H.; Kumar, D.; Thiel, W. *Chem. Rev.* **2010**, *110*, 949−1017.
(11) Shaik, S.; Hirao, H.; Kumar, D. *Nat. Prod. Rep.* **2007**, *24*, 533−552.
(12) Shaik, S.; Hirao, H.; Kumar, D. *Acc. Chem. Res.* **2007**, *40*, 532−542.
(13) Murray, M. *Curr. Drug Metab.* **2000**, *1*, 67−84.
(14) Kent, U. M.; Jushchyshyn, M. I.; Hollenberg, P. F. *Curr. Drug Metab.* **2001**, *2*, 215−243.
(15) Hollenberg, P. F.; Kent, U. M.; Bumpus, N. N. *Chem. Res. Toxicol.* **2008**, *21*, 189−205.
(16) Zhou, S.; Chan, S. Y.; Goh, B. C.; Chan, E.; Duan, W.; Huang, M.; McLeod, H. L. *Clin. Pharmacokinet.* **2005**, *44*, 279−304.
(17) Zhou, S. *Curr. Drug Metab.* **2008**, *9*, 310−322.
(18) Pelkonen, O.; Turpeinen, M.; Hakkola, J.; Honkakoski, P.; Hukkanen, J.; Raunio, H. *Arch. Toxicol.* **2008**, *82*, 667−715.
(19) Lin, J. H.; Lu, A. Y. H. *Clin. Pharmacokinet.* **1998**, *35*, 361−390.

DOI: 10.1021/acscatal.5b00423
ACS Catal. 2015, 5, 2952−2960

(20) Orr, S. T. M.; Ripp, S. L.; Ballard, T. E.; Henderson, J. L.; Scott, D. O.; Obach, R. S.; Sun, H.; Kalgutkar, A. S. *J. Med. Chem.* **2012**, *55*, 4896−4933.
(21) Kamel, A.; Harriman, S. *Drug Discovery Today: Technol.* **2013**, *10*, e177−e189.
(22) Fontana, E.; Dansette, P. M.; Poli, S. M. *Curr. Drug Metab.* **2005**, *6*, 413−454.
(23) Hirao, H.; Cheong, Z. H.; Wang, X. *J. Phys. Chem. B* **2012**, *116*, 7787−7794.
(24) Hirao, H.; Chuanprasit, P.; Cheong, Y. Y.; Wang, X. *Chem. - Eur. J.* **2013**, *19*, 7361−7369.
(25) Hirao, H.; Thellamurege, N.; Chuanprasit, P.; Xu, K. *Int. J. Mol. Sci.* **2013**, *14*, 24692−24705.
(26) de Visser, S. P.; Kumar, D.; Shaik, S. *J. Inorg. Biochem.* **2004**, *98*, 1183−1193.
(27) Taxak, N.; Desai, P. V.; Patel, B.; Mohutsky, M.; Klimkowski, V. J.; Gombar, V.; Bharatam, P. V. *J. Comput. Chem.* **2012**, *33*, 1740−1747.
(28) Taxak, N.; Patel, B.; Bharatam, P. V. *Inorg. Chem.* **2013**, *52*, 5097−5109.
(29) Taxak, N.; Kalra, S.; Bharatam, P. V. *Inorg. Chem.* **2013**, *52*, 13496−13508.
(30) Williams, J. A.; Hurst, S. I.; Bauman, J.; Jones, B. C.; Hyland, R.; Gibbs, J. P.; Obach, R. S.; Ball, S. E. *Curr. Drug Metab.* **2003**, *4*, 527−534.
(31) Kostrubsky, S. E.; Strom, S. C.; Kalgutkar, A. S.; Kulkarni, S.; Atherton, J.; Mireles, R.; Feng, B.; Kubik, R.; Hanson, J.; Urda, E.; Mutlib, A. E. *Toxicol. Sci.* **2006**, *90*, 451−459.
(32) Linder, C. D.; Renaud, N. A.; Hutzler, J. M. *Drug Metab. Dispos.* **2009**, *37*, 10−13.
(33) Strelevitz, T. J.; Foti, R. S.; Fisher, M. B. *J. Pharm. Sci.* **2006**, *95*, 1334−1341.
(34) Ortiz de Montellano, P. R.; Mico, B. A.; Mathews, J. M.; Kunze, K. L.; Miwa, G. T.; Lu, A. Y. *Arch. Biochem. Biophys.* **1981**, *210*, 717−728.
(35) Ortiz de Montellano, P. R.; Mathews, J. M. *Biochem. J.* **1981**, *195*, 761−764.
(36) Ortiz de Montellano, P. R.; Mathews, J. M.; Langry, K. C. *Tetrahedron* **1984**, *40*, 511−519.
(37) Mathews, J. M.; Bend, J. R. *Mol. Pharmacol.* **1986**, *30*, 25−32.
(38) Woodcroft, K. J.; Bend, J. R. *Can. J. Physiol. Pharmacol.* **1990**, *68*, 1278−1285.
(39) Woodcroft, K. J.; Webb, C. D.; Yao, M.; Weedon, A. C.; Bend, J. R. *Chem. Res. Toxicol.* **1997**, *10*, 589−599.
(40) Kent, U. M.; Bend, J. R.; Chamberlin, B. A.; Gage, D. A.; Hollenberg, P. F. *Chem. Res. Toxicol.* **1997**, *10*, 600−608.
(41) Frisch, M. J.; Trucks, G. W.; Schlegel, H. B.; Scuseria, G. E.; Robb, M. A.; Cheeseman, J. R.; Scalmani, G.; Barone, V.; Mennucci, B.; Petersson, G. A.; Nakatsuji, H.; Caricato, M.; Li, X.; Hratchian, H. P.; Izmaylov, A. F.; Bloino, J.; Zheng, G.; Sonnenberg, J. L.; Hada, M.; Ehara, M.; Toyota, K.; Fukuda, R.; Hasegawa, J.; Ishida, M.; Nakajima, T.; Honda, Y.; Kitao, O.; Nakai, H.; Vreven, T.; Montgomery, J. A., Jr.; Peralta, J. E.; Ogliaro, F.; Bearpark, M.; Heyd, J. J.; Brothers, E.; Kudin, K. N.; Staroverov, V. N.; Kobayashi, R.; Normand, J.; Raghavachari, K.; Rendell, A.; Burant, J. C.; Iyengar, S. S.; Tomasi, J.; Cossi, M.; Rega, N.; Millam, J. M.; Klene, M.; Knox, J. E.; Cross, J. B.; Bakken, V.; Adamo, C.; Jaramillo, J.; Gomperts, R.; Stratmann, R. E.; Yazyev, O.; Austin, A. J.; Cammi, R.; Pomelli, C.; Ochterski, J. W.; Martin, R. L.; Morokuma, K.; Zakrzewski, V. G.; Voth, G. A.; Salvador, P.; Dannenberg, J. J.; Dapprich, S.; Daniels, A. D.; Farkas, O.; Foresman, J. B.; Ortiz, J. V.; Cioslowski, J.; Fox, D. J. *Gaussian 09*, revision B.01; Gaussian, Inc.: Wallingford, CT, 2010.
(42) Becke, A. D. *J. Chem. Phys.* **1993**, *98*, 5648−5652.
(43) Lee, C.; Yang, W.; Parr, R. G. *Phys. Rev. B: Condens. Matter Mater. Phys.* **1988**, *37*, 785−789.
(44) Vosko, S. H.; Wilk, L.; Nusair, M. *Can. J. Phys.* **1980**, *58*, 1200−1211.
(45) Dolg, M.; Wedig, U.; Stoll, H.; Preuss, H. *J. Chem. Phys.* **1987**, *86*, 866−868.
(46) Hehre, W. J.; Radom, L.; Schleyer, P. v. R.; Pople, J. A. *Ab Initio Molecular Orbital Theory*; Wiley, New York, 1986; Vol. *67*.
(47) Krishnan, R.; Binkley, J. S.; Seeger, R.; Pople, J. A. *J. Chem. Phys.* **1980**, *72*, 650−656.
(48) Hariharan, P. C.; Pople, J. A. *Theor. Chim. Acta* **1973**, *28*, 213−222.
(49) Clark, T.; Chandrasekhar, J.; Spitznagel, G. W.; Schleyer, P. v. R. *J. Comput. Chem.* **1983**, *4*, 294−301.
(50) Tomasi, J.; Mennucci, B.; Cammi, R. *Chem. Rev.* **2005**, *105*, 2999−3094.
(51) Curtiss, L. A.; Redfern, P. C.; Raghavachari, K. *J. Chem. Phys.* **2007**, *126*, 084108−084113.
(52) de Visser, S. P. *J. Am. Chem. Soc.* **2010**, *132*, 1087−1097.
(53) Pettersen, E. F.; Goddard, T. D.; Huang, C. C.; Couch, G. S.; Greenblatt, D. M.; Meng, E. C.; Ferrin, T. E. *J. Comput. Chem.* **2004**, *25*, 1605−1612.
(54) Portmann, S.; Lüthi, H. P. *CHIMIA* **2000**, *54*, 766−770.
(55) Hirao, H.; Chuanprasit, P. *Chem. Phys. Lett.* **2015**, *621*, 188−192.
(56) de Visser, S. P.; Shaik, S. *J. Am. Chem. Soc.* **2003**, *125*, 7413−7424.
(57) Usharani, D.; Lacy, D. C.; Borovik, A. S.; Shaik, S. *J. Am. Chem. Soc.* **2013**, *135*, 17090−17104.
(58) Chen, H.; Murray, J.; Kornberg, B.; Dethloff, L.; Rock, D.; Nikam, S.; Mutlib, A. E. *Chem. Res. Toxicol.* **2006**, *19*, 1341−1350.
(59) Wang, Y.; Hirao, H.; Chen, H.; Onaka, H.; Nagano, S.; Shaik, S. *J. Am. Chem. Soc.* **2008**, *130*, 7170−7171.
(60) de Visser, S. P.; Tan, L. S. *J. Am. Chem. Soc.* **2008**, *130*, 12961−12974.
(61) Kumar, S.; Faponle, A. S.; Barman, P.; Vardhaman, A. K.; Sastri, C. V.; Kumar, D.; de Visser, S. P. *J. Am. Chem. Soc.* **2014**, *136*, 17102−17115.

DOI: 10.1021/acscatal.5b00423
ACS Catal. 2015, 5, 2952−2960